Temperature dependence of photoluminescence bands in $Zn_{1-x}Cd_xSe/ZnSe$ quantum wells with planar CdSe islands

A. Klochikhin,* A. Reznitsky,† B. Dal Don, H. Priller, H. Kalt, and C. Klingshirn
Institut für Angewandte Physik, Universität Karlsruhe (TH), 76128 Karlsruhe, Germany

S. Permogorov and S. Ivanov
A.F. Ioffe Physical-Technical Institute, 194021, St. Petersburg, Russia
(Received 20 August 2003; published 18 February 2004)

We have studied the temperature dependence of the photoluminescence (PL) spectra of molecular beam epitaxy grown ultrathin $Zn_{1-x}Cd_xSe/ZnSe$ quantum wells with random and inhomogeneous Cd distributions over cation sublattice within the temperature interval 2–300 K. Depending on the Cd concentration, the PL band maximum position $E_{max}^{PL}(T)$ follows either a ''normal'' or an ''anomalous'' (known as ''S-shaped'') temperature dependence. We have analyzed both dependences in detail for a model of an island ensemble which can be characterized by a single-mode distribution of the most important parameters governing the optical properties of the quantum well. We demonstrate that the anomalous behavior arises due to the strong temperature dependence of the lifetimes of a family of metastable states participating in formation of the PL band at low temperatures. The metastablility of some island states is ascribed to a complex topological structure of the islands. The mechanism of the exciton-phonon interaction responsible for the fast decrease of the lifetime of these states with the increase of temperature has the same origin as the mechanism leading to the vanishing of narrow lines in μ-PL. We also present results of time-resolved experiments which yield the shift of the PL band for hot excitons cooling in a cold lattice.

DOI: 10.1103/PhysRevB.69.085308 PACS number(s): 78.55.Et, 73.21.Fg, 78.67.De

I. INTRODUCTION

The effect of temperature on the exciton photoluminescence (PL) provides important information on the exciton-phonon interaction both in regular semiconductor crystals and in their solid solutions and presents a convenient tool for probing the exciton kinetics. For free excitons in many pure II-VI semiconductors the luminescence bands are strongly dependent on the sample temperature. With a temperature increase the average kinetic energy of excitons increases, the exciton-phonon luminescence replicas broaden, and their maxima shift in the high energy direction. The shapes of replicas reflect the equilibrium distribution of excitons over their kinetic energies in the ground state.[1] At the same time the line of resonant luminescence strictly follows the band-gap narrowing. The observed shift of the exciton–LO-phonon luminescence band maximum results from the interplay of these factors.

In solid solutions the interband luminescence occurs from the tails of localized states produced by composition fluctuations.[2] Most efficient in luminescence are the so-called emitting localized states which are spatially isolated from other states and have no means of a nonradiative relaxation.[3] The luminescence bands are positioned below the band gap or absorption maximum of the ground exciton state. The temperature increase leads to an increase of the population of higher states, to a broadening of the luminescence bands, and to a monotonic shift of the PL band towards the absorption maximum.

For quantum wells (QWs) formed of ternary solid solutions with strongly mismatched lattices, the homogeneous random distribution of solute atoms becomes unstable at relatively small concentrations. As a result, in the QW plane islands of nanometer scale appear, for which the content of the narrow-gap component essentially exceeds the average value for QW. It is generally believed that the formation of islands allows to reduce the internal strains arising from the lattice misfit between adjacent layers.[4]

Fractional monolayer insertions of CdSe in ZnSe have been investigated in many works.[5–30] When the total deposited amount of CdSe exceeds about 0.5 ML the resulting $Zn_{1-x}Cd_xSe$ QWs are inhomogeneous systems incorporating islands enriched in CdSe content.[7] These islands can differ in size, spatial configuration, and in the excess Cd concentration. The island sizes and the distances between the islands, the Cd content within and between the islands, as well as the dispersion of these values, can be estimated from the structural data, obtained, for example, by the high resolution transmission electron microscopy[10–15] (HRTEM) or by the high resolution x-ray diffraction.[19–21]

The feature distinguishing the disorder of the system with islands in an ultrathin QW from that in an random solid solution is the spatial size of fluctuations. The composition fluctuations in random solid solutions form a potential relief for excitons due to a random or nearly random distribution of the substitution atoms over the lattice sites. The most important potential wells for exciton localization have a minimal size which is sufficient for the creation of a single bound state. The appearance of a potential well containing more than one localized state is rather improbable statistically because this implies a significant increase of the fluctuation size.[31]

In QWs with islands the large lateral size of quantum islands and the considerable difference of Cd concentration in and between the islands lead to a rich spectrum of localized exciton states. The spectrum of exciton states in an is-

land depends on the size of the island as long as the number of states in the island is small. However, the estimates[32] show that if the lateral size of the $Zn_{1-x}Cd_xSe$ islands exceeds ≈ 5 nm the energy position of the deepest states become almost independent of the island size. The variations of the concentration are much more efficient and lead to strong inhomogeneous broadening of the energy spectra.

Many publications were devoted to the temperature dependence of the PL-band maximum in two-dimensional systems.[33–43] In many cases this dependence at low temperatures demonstrates a redshift of the PL maximum with the temperature increase with respect to absorption or the PL excitation (PLE) maximum.[33–43] In such cases, the temperature dependence of the Stokes shift has an anomalous or so-called S-shaped character, i.e., it passes through a minimum with the increase of temperature.

An anomalous behavior of the Stokes shift was observed for $Zn_{1-x}Cd_xSe/ZnSe$ QWs grown by different epitaxial techniques, a few examples can be found in Refs. 17 and 44–48. The most puzzling feature of the anomalous behavior in these systems is a large value of the low temperature redshift which is sometimes significantly larger than the thermal energy at the temperature at which the shift occurs.

The physical mechanisms and parameters which govern this anomalous behavior are still under discussion.[29,35,41,42,44,49] A stationary temperature-dependent solution for the exciton distribution over localized states was obtained in Refs. 35 and 41. However, in both works the distribution demonstrates an inappropriate behavior in the low temperature limit $T \rightarrow 0$. A theoretical model which takes into account the exciton radiative decay and the exciton-phonon relaxation was developed in Ref. 42. In Refs. 29 and 44 it has been assumed that in $Zn_{1-x}Cd_xSe/ZnSe$ QWs with nanoislands the exciton relaxation has inter-island character. At the same time, recent Monte Carlo simulations of exciton tunneling relaxation indicate a relaxation only within the islands.[49] It is worth noting that very different models of Refs. 42 and 49 both have a strong dependence of the results on parameters of the exciton-phonon interaction. However, only a qualitative agreement with experimental data has been achieved in Refs. 42 and 49. The dependence of the exciton distribution on the details of the exciton-phonon interaction suggests a nonequilibrium character of the distribution of localized excitons in contrast to the case of free excitons.[1] On the other hand, the normal monotonic type of temperature dependence for the Stokes shift for the luminescence of localized exciton can be expected for the thermal equilibrium redistribution of the population. The difference between normal and anomalous dependences is essential only at low temperatures while in the high temperature limit in both cases the PL band maximum tends to the absorption maximum. Therefore, the question arises whether or not the equilibrium population can produce the anomalous Stokes shift.

The aim of this paper is an experimental study of the temperature dependence of the Stokes shift between PL and PLE maxima in $Zn_{1-x}Cd_xSe/ZnSe$ QWs with nanoislands at cw and pulse excitation, and the development of the theoretical approach which assumes the equilibrium distribution of excitons over the localized states of islands. We show that the redshift of the PL maximum indicates that an appreciable part of the emitting states of excitons in nanoislands at the lowest temperatures are metastable states[46] which can relax to deeper states as the temperature increases. We consider some simple models of island ensembles which describe the appearance of the metastable states. We assign the temperature dependence of the lifetime of the metastable states in the low temperature interval to the new multiphonon mechanism. This mechanism is similar to that used early to explain the disappearance of the narrow lines out of the μ-PL spectra.[5,23,27,44,50]

The structure of the paper is as follows. In Sec. II we describe the details of the experiment. We study $Zn_{1-x}Cd_xSe/ZnSe$ systems with planer CdSe islands appearing within $Zn_{1-x}Cd_xSe$ quantum wells. Section III presents the typical normal and anomalous temperature shifts of the PL-band maxima. In discussions of our results we restrict ourselves to a single mode quantum island ensemble. We also present the results of time-resolved studies of the shift of the PL band maximum. In Sec. IV we develop a model approach in order to find the optical characteristics of exciton states averaged over a single mode quantum island ensemble. We also consider the exciton-phonon interaction in islands to solve the problem of the anomalous temperature shift of the photoluminescence band and to establish an interrelation of this problem with the low temperature decrease of the narrow lines in the μ-PL spectra. In the last section we summarize the results obtained in the paper.

II. EXPERIMENTAL DETAILS AND RESULTS

A. Samples

We have studied steady-state and time-resolved PL as well as steady-state PLE spectra of two systems.

(i) Single QWs grown in migration enhanced epitaxy (MEE) mode by cycled deposition of CdSe (by 0.3 ML per cycle) in ZnSe matrices. The representative set of samples with the following number of cycles: 1, 2, 5, 8, and 10 was used.

(ii) Single QWs grown by modified molecular beam epitaxy (MBE) techniques with a CdS source for supplying Cd atoms. The nominal CdSe content in QW ranges from 1.5 to 3.2 ML (for more growth details see Refs. 7 and 51.

As established by HRTEM data, QWs in both studied sets of samples consist of $Zn_{1-x}Cd_xSe$ solid solutions with the mean width of the QW of about 5–10 ML. The width of QW is defined by the growth technique and practically does not depend on the total amount of deposited CdSe.[14,18]

Further we present the results on two particular samples named *Mee*1 (a MEE grown $Zn_{1-x}Cd_xSe$ QW with a nominal Cd thickness of 0.6 ML) and *Mbe*1 (a MBE grown $Zn_{1-x}Cd_xSe$ QW with the nominal Cd thickness of 2 ML). The sample *Mbe*1 consists of a $Zn_{1-x}Cd_xSe$ quantum film with Cd-rich regions, forming the islands. The islands have lateral dimensions from 5 to 10 nm, and their density is evaluated to be about 5×10^{11} cm^{-2}. In sample *Mee*1 the distribution of Cd in quantum film is homogeneous and can be considered as random.

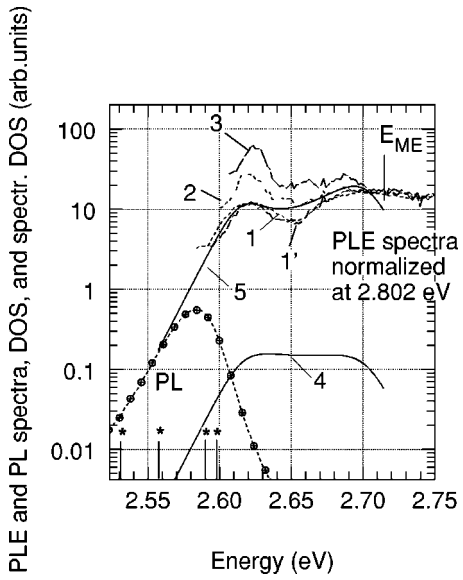

FIG. 1. PL and PLE spectra of the sample $Mbe1$ at 5 K. Curves 1, 1', 2, and 3 are the PLE spectra detected at different positions in the PL band (decorated curve). Corresponding detector positions for these spectra are shown by vertical lines with asterisks. The position of the mobility edge is denoted as E_{ME} (see text). Curve 4 is the model density of states (DOS) of the exciton localized in the island. Curve 5 is the corresponding spectral DOS of the localized excitons.

B. Experimental setup and optical characterization of a sample

The 441.6-nm (2.81-eV) or 325-nm (3.81-eV) lines of a He-Cd laser were used for the excitation of PL spectra. PLE spectra were studied using the emission from a Xe lamp dispersed by a monochromator. In time-resolved spectroscopy we used frequency-doubled pulses from a Ti-saphire laser for excitation with a pulse length of about 150 fs, a spectral width of about 10 meV, and a repetition rate of 76 MHz. A synchroscan streak camera coupled to a spectrometer was used for detection. The spectral and time resolutions of the detection system were about 0.5 meV and 6 ps, respectively.

A set of PLE spectra of sample $Mbe1$ is presented in Fig. 1. The PLE spectra were obtained for different detector positions in the PL band and were normalized at an energy of 2.80 eV, slightly below the exciton transition of ZnSe.[30] After such a normalization, the PLE spectra coincide in a wide range above some energy E_{ME}. This fact proves that the relaxation times of all states excited above E_{ME} are much shorter than the lifetimes of all emitting states.

As it can be seen from Fig. 1, at $\hbar\omega < E_{ME}$ the PLE curves exhibit a strong dependence on the detection energy. The PL band shape and its maximum position also change when exciting below E_{ME} as compared with the excitation above this energy (see Fig. 4). Therefore, both PL and PLE spectra show that different ensembles of the exciton states are excited above and below the energy E_{ME}. They differ considerably with respect to their relaxation properties. This difference can be understood if we assume that the excitons above the energy E_{ME} are mobile and can be trapped, first of all, by the largest islands, which have the largest cross section of the trapping process while the excitation below E_{ME} creates excitons in a random ensemble of islands having electronic levels at proper energy. The latter ensemble has an average, relaxation properties different from ones of the most effective traps. This difference allows us to regard E_{ME} as the mobility edge for excitons in QW with islands.[30]

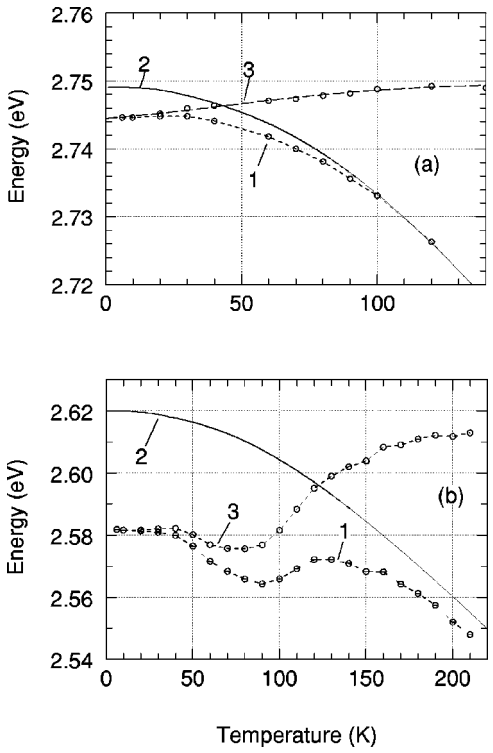

FIG. 2. Temperature shift of the PL band maximum. (a) Curve 1 present experimental data for the sample $Mee1$. Solid line 2 is the temperature behavior of the PLE maximum approximated by the ZnSe band gap dependence $\Delta E_G(T)$. Curve 3 present the data of curve 1 after subtraction of the band gap shrinkage $\Delta E_G(T)$. (b) The same as in (a) for the sample $Mbe1$.

The PLE spectra of the states forming the low energy part of the PL band do not depend on the detector position even for $E < E_{ME}$ and coincide with high accuracy (see the two curves labeled by 1 and 1' in Fig. 1). This means that the PL band in this energy interval is formed by the states which are not subjected to further energy relaxation, so that they can be considered as the ground states of the islands. For this reason, the PLE spectra detected at the low energy side of the PL band are expected to reproduce the absorption spectrum of excitons in the islands.

III. NORMAL AND ANOMALOUS TEMPERATURE SHIFT OF THE PL BAND AT CW EXCITATION

In Fig. 2(a) the temperature dependence of the PL band maximum position $E_{PL}^{max}(T)$ of a QW formed by diluted $Zn_{1-x}Cd_xSe$ solid solutions is shown (sample $Mee1$). For diluted solid solutions the maximum of the PL band $E_{PL}^{max}(T)$ (curve 1) follows a temperature dependence which we shall call normal. When the temperature increases, $E_{PL}^{max}(T)$ shifts monotonically to the band gap temperature dependence

(curve 2). It is seen that curve 3 in Fig. 2(a) obtained from the data presented by curve 1 by means of subtraction of the band gap shrinkage $\Delta E_G(T)$ tends to the PLE maximum position at $T=0$.

The temperature behavior of the PL band maximum for sample $Mbe1$ with nanoislands is demonstrated in Fig. 2(b). Though the PL band maximum $E_{PL}^{max}(T)$ has, in general, the same tendency as in the previous case to move toward the curve $E_G(T)$ its behavior is characterized by the dip at the temperature of about 80 K. It is seen from Fig. 2(b) that after the subtraction of $\Delta E_G(T)$ the obtained result [curve 3 in Fig. 2(b)] differs considerably from the normal behavior.

A. Temperature shift of the band gap in a regular crystal

The temperature dependence of the band gap $E_G(T)$ or of the exciton ground state energy (for simplicity, we do not distinguish between these two items) results from the electron and hole interaction with lattice vibrations and from the thermal expansion of the crystal lattice. A theoretical treatment of this problem was presented in Refs. 52 and 53. Two mentioned mechanisms are also responsible for the band gap shrinkage in nanosystems, as demonstrated in Ref. 54.

Beyond the straightforward theory in literature there is a number of empirical equations which allow one to fit the experimental dependence of $\Delta E_G(T)=E_G(T)-E_G(0)$.[55–59] We have found that the dependence $E_G(T)$ for ZnSe bulk material can be well fitted by the sum of two terms proportional to the phonon occupation numbers: the first one with the Debye temperature Θ_D of the host lattice and the second with $\Theta_{eff}\approx 0.2\Theta_D$, corresponding to the interaction with optical and acoustical phonons, respectively:

$$\Delta E_G(T)=-\alpha N(\Theta_{eff})-\gamma N(\Theta_D), \tag{1}$$

where

$$N(\Theta)=[exp(\Theta/T)-1]^{-1}, \tag{2}$$

and $\Theta=\Theta_D$ or Θ_{eff}.

To describe the $\Delta E_G(T)$ in Figs. 2(a) and 2(b) we have used Eq. (1) with parameters for free exciton transitions of ZnSe ($\Theta_D=270$ K,[60] $\Theta_{eff}=54$ K, $\alpha=0.005$ eV, and $\gamma=0.0888$ eV). The obtained curve is shifted to fit the position of corresponding PLE maximum [curves 2 in Figs. 2(a) and 2(b)].

B. Thermal population of excited states in random solid solutions and in islands

We denote the difference in energies of absorption and luminescence band maxima at zero temperature as

$$\Delta E_S=E_{PLE}^{max}(0)-E_{PL}^{max}(0), \tag{3}$$

where $E_{PLE}^{max}(0)$ and $E_{PL}^{max}(0)$ are the energies of absorption and emission maxima. We assume that the temperature shift of absorption maximum coincides with the shift of $\Delta E_G(T)$:

$$E_{PLE}^{max}(T)=E_{PLE}^{max}(0)+\Delta E_G(T). \tag{4}$$

The temperature shift of the PL band maximum $E_{PL}^{max}(T)$ is determined by three terms. The first of them is common for the absorption and emission processes and is related to the band gap dependence $E_G(T)$. This process does not shift the emission with respect to the absorption.

The second term is temperature dependent classical Stokes shift of absorption and emission in opposite directions due to phonon assisted processes. This term is not very important for the exciton states in quantum islands which are characterized by the relatively weak exciton-phonon interaction and can be neglected. The third term is inherent to disordered systems and arises from the thermal redistribution of population between ground and excited states.

(1) The luminescence of random solid solutions at lowest temperatures is formed by the spatially isolated states which have no ways for exciton-phonon transition into lower states.[3] The density of states (DOS) of spatially isolated states $\rho_{isol}(\omega)$[3] can be found with the help of classical percolation theory,

$$\rho_{isol}(\omega)=\rho(\omega)\exp[-\beta N(\omega)/N(E_{ME})], \tag{5}$$

where $\rho(\omega)$ is the density of localized states and the value of β is known for different continuum systems. It has the order of unity and depends on the dimensionality of disordered system.[61] $N(\omega)$ is the integrated number of localized states below ω. The luminescence intensity is proportional to the spectral DOS of these states and the maximum $E_{PL}^{max}(0)$ occurs just below the percolation threshold E_{ME}.

In case of weak cw excitation we can use the Gibbs statistics for the equilibrium population of the excited states in every island. Then the average population of the localized states in island ensemble $p(\omega,T)$ can be written as

$$p(\omega,T)\sim Z^{-1}(T)\left\langle \rho_{isol}(\omega)+\int_{-\infty}^{\omega} d\omega_1[\rho_{isol}(\omega_1)/\overline{\rho_{isol}}] \times[\rho(\omega)-\rho_{isol}(\omega)]\exp\{-\hbar(\omega-\omega_1)/T\}\right\rangle. \tag{6}$$

Here, $\overline{\rho_{isol}}=\int_{-\infty}^{\infty} d\omega\rho_{isol}(\omega)$, and $Z=\int_{-\infty}^{\infty} d\omega\langle\cdots\rangle$ where the angle brackets $\langle\cdots\rangle$ contain the same expression as in Eq. (6).

The function $p(\omega,T)$ has the especially simple behavior at $T\to 0$ and $T\to\infty$. In the limit $T\to 0$ the population $p(\omega,T)\sim\rho_{isol}(\omega)$. These spatially isolated states should be taken into account to maintain the equilibrium population because they play a role of ground states in a disordered system. In the limit $T\to\infty$ all states are equally populated, and $p(\omega,T)\sim\rho(\omega)$.

According to Eq. (6), the thermal population of excited states spreads monotonously to the blue at increasing the temperature. The same character we can expect for the behavior of the PL band until its maximum reaches the position of the zero-phonon band of the spectral DOS, i.e., the absorption band maximum. A further increase of the population of higher states should not shift the PL band maximum be-

cause the oscillator strength of these states rapidly drops. As a result, $E_{PL}^{max}(T)$ should follow the $E_G(T)$ dependence in the high temperature limit.

(2) In the case of QWs with islands the PL band is far below the mobility edge of the QW. It is formed by the tail states of the band which is observed in PLE spectra as the low energy maximum.

In order to explain the origin of the anomalous temperature shift of the PL band in QWs with islands we assume that the PL band and the low energy PLE band are formed by a entire group of states in every island. These states differ in the energy position and in the spatial extent of the wave functions. The low energy PLE band maximum is formed by the highest states from this group. The lowest states are spatially isolated from each other and have the lifetime restricted by the radiative recombination. The intermediate and highest states of this group have the possibility for the relaxation with the phonon emission.

In the case of islands we introduce two energies E_{isol} and $E_{mts}>E_{isol}$ for the averaged characterization of the island ensemble (index *mts* stands for metastable states). The energy E_{isol} we define as an average upper border of spatially isolated states in the island system and the energy $E_{mts}(0)$ as an average upper border of all isolated plus metastable states forming the PL band at zero temperature. Taking into account that islands form a disordered system, we present the averaged density of spatially isolated states again in the form of Eq. (5), where now $\rho(\omega)$ is the average density of states localized in islands, β is a parameter of the order of unity and $N(\omega)$ is an average integrated density of states below ω in the island ensemble. The similar form we assume for the averaged density of all isolated plus metastable states at a finite temperature, namely,

$$\rho_{isol+mts}(\omega,T)=\rho(\omega)\exp[-\beta N(\omega)/N[E_{mts}(T)]]. \quad (7)$$

This equation gives the density of states which can be thermally activated. We can express the temperature dependent border position of the metastable states as

$$E_{mts}(T)=(E_{mts}(0)-\delta E\{1-\exp[-\tau_{em}w_{rel}(T)]\}), \quad (8)$$

where $\delta E=[E_{mts}(0)-E_{isol}]$, and $w_{rel}(T)$ is an average relaxation probability for the metastable states and τ_{em} is the lifetime of the radiative recombination. The metastable states participate in the PL band formation until $[\tau_{em}w_{rel}(T)]<1$. They disappear from luminescence at some temperature in the limit $[\tau_{em}w_{rel}(T)]\gg 1$ if they are not thermally populated at this temperature.

For the thermal population of the excited states we can again use Eq. (6), substituting $\rho_{isol+mts}(\omega,T)$ for $\rho_{isol}(\omega)$. The temperature increase in this case causes, on the one hand, the thermal activation of the higher states and, on the other hand, the shift of the border of the metastable states toward the border of isolated states E_{isol} which is independent on the temperature. These two processes shift the PL band maximum in opposite directions. If there exists a temperature interval where the shift of the border of the metastable states is dominant the PL band will shift toward low energies. Results of calculations of the DOS and of the spectral DOS of the exciton states localized in the island using parameters appropriate for the sample $Mbe1$ are shown in Fig. 1.

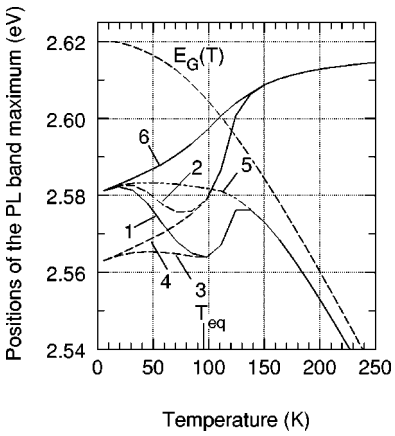

FIG. 3. Results of model calculations of the temperature shift of the PL band maximum in different limits. Curve 1 is anomalous shift for $[\tau_{em}w_{rel}(T)]\sim T^{3.5}$, curve 2 is the same after subtraction of the band gap shrinkage $\Delta E_G(T)$, curve 3 present the normal shift in the limit of very fast relaxation of metastable states $(\tau_{em}w_{rel}(T))\to\infty$, curve 4 is the same after subtraction of $\Delta E_G(T)$. Curve 5 is the normal shift in the limit of nonrelaxing metastable states $(\tau_{em}w_{rel}(T))\to 0$, and curve 6 is the same after subtraction of $\Delta E_G(T)$. T_{eq} denotes the temperature above which only the equilibrium population of excited states is responsible for the shift.

Results of model calculations of the shift of the maximum of the spectral DOS of populated states (PL band maximum) are presented in Fig. 3. Curve 1 demonstrates the anomalous behavior due to the temperature dependence of the lifetime of metastable states. Curves 3 and 4 give an example of the normal shift which was obtained in the limit of the very fast relaxation of the metastable states. Curve 5 exhibits the normal dependence in the limit of very slow relaxation of the metastable states. Details of these calculations are described in Sec. IV.

Figure 4 shows the low temperature shapes of the PL bands at different excitation energies together with results of model calculations of the spectral DOS of isolated and isolated plus metastable states, the densities of which $\rho_{isol}(\omega)$ and $\rho_{isol+mts}(\omega,T=0)$ are given by Eqs. (5) and (8), respectively, with $\beta=1$. In these calculations we have used the energies E_{isol} and E_{mts} as fitting parameters. The energy parameter $E_{mts}(0)$ is found by fitting the PL band shape, using the spectral DOS of the states given by Eq. (7) and the model DOS $\rho(\omega)$ derived in Sec. IV. The parameter $E_{isol}(0)$ was defined by fitting the shift of the PL band maximum in the high temperature limit $[\tau_{em}w_{rel}(T)]\gg 1$.

C. Shift of the PL-band maximum at pulse excitation

A fast increase of the relaxation probability of the metastable states $w_{rel}(T)$ at low temperatures can explain the low-energy shift of the PL band maximum in the temperature interval where the normal part of the shift is relatively small. The only reason for the fast decrease of the lifetime of the

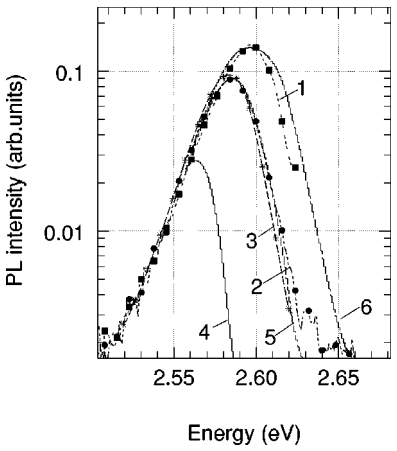

FIG. 4. (a) PL spectra of the sample $Mbe1$ at the temperature $T=5$ K for excitation energies 2.641 (curve 1) and 2.779 eV (curve 2). Curve 3 is the PL spectrum at cw excitation above the ZnSe band gap. Curve 4 is the spectral DOSs of the exciton ground states in island calculated in Sec. IV. Curves 5 and 6 are the spectral DOSs of exciton at different positions of E_{mts} calculated in Sec. IV.

metastable states can be an increase of the exciton-phonon relaxation rate with temperature. The time-resolved spectroscopy gives a possibility to exclude the temperature effect on the exciton relaxation rate.

Figure 5(a) demonstrates the results of the pulsed excitation experiment. The shape of the PL band shows that hot excitons are distributed over an energy interval depending on the time delay. A monotonic shift of the PL band maximum occurs with a time delay increase, which represents the exciton relaxation in the cold lattice. In this case we can suppose that the metastable states do not relax during the observation time which corresponds to the limiting case $[\tau_{em}w_{rel}(T)]\rightarrow 0$. Curve 5 in Fig. 3 demonstrates results of the model calculations of the shift of the PL band maximum in this limit.

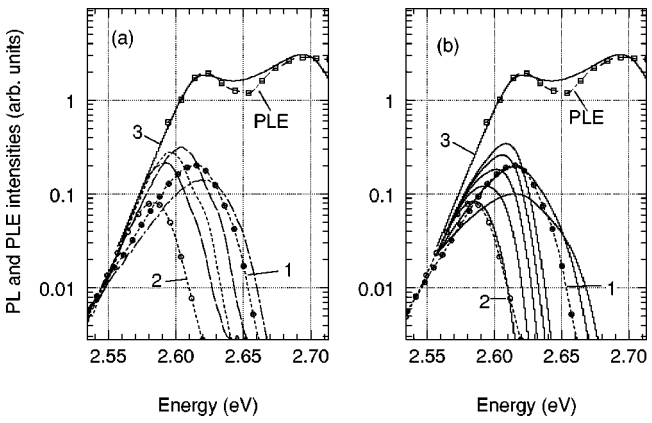

FIG. 5. (a) Time resolved PL spectra of the sample $Mbe1$. at 5 K. The signal was integrated over 10 ps for every time delay. Time delay for experimental curves in the order of red shift is $\Delta t=0$, 50, 100, 200, 400, and 600 ps, respectively. The last curve coincides with the PL spectrum at cw excitation. Decorated curves 1 and 2 are the time resolved spectra at $\Delta t=50$ and 600 ps. They are also presented in (b) for comparison. Curve 3 is the calculated spectral DOS simulating the PLE spectrum. (b) The set of solid lines present the calculated PL spectra of excitons at different effective temperatures. Curves 1, 2, and 3 and the PLE spectrum are the same as in (a).

The model calculations of Sec. IV presented in Fig. 5(b) show that the position of the corresponding PL band maximum at every time delay can be characterized by some effective temperature T^* which can be determined from a comparison of observed and calculated PL band positions.

The shift of the PL band maximum as a function of T^* has a monotonic normal-like character for the same sample, which shows the anomalous dependence in the temperature interval from 5 to 250 K while heating or cooling the sample. Thus, the key issues for the explanation of the anomalous temperature shift are the questions (i) why and how do the metastable states arise at least in some islands, and (ii) why do they disappear from emission already at relatively low temperatures. These two problems are treated in Sec. IV.

IV. AVERAGED CHARACTERISTICS OF EXCITON STATES IN AN ISLAND ENSEMBLE

A. Statistical models of island ensembles

The influences of the lateral shape of the island on the spectrum and on the luminescence characteristics were not investigated properly till now. There are different reasons which can lead to the formation of different lateral shapes for islands. The first reason is simply statistical. Even if we consider an ensemble of identical ''unit'' islands, their random distribution in space will create a number of island clusters which can be treated as islands of different sizes and different lateral shapes. The exciton relaxation rate from a state into some deepest state will sharply decrease if, for example, these two states are positioned in different islands of the cluster of two weakly overlapping islands. Therefore, we can expect a qualitative change of the relaxation rate for the part of exciton states localized in island complexes as compared with the isolated islands. That is, in such complex islands appears the possibility of a space separation of the wave functions and of a slow nonradiative relaxation of the excitons in excited states.

Let us consider a QW containing $n=10^{11}$ cm^{-2} islands which have, in the lateral plane, the shape of disks with a diameter equal to 10 nm. We assume that the entire lateral plane of a QW is divided into square cells with the side equal to $L=10$ nm, so that the number of cells on the unit area is $N=(1/L)^2=10^{12}$ cm^{-2}, and an island can be placed only in a cell. The concentration of islands in the sample is $c=n/N=0.1$ or 10% of the cells will be filled by islands. Each of the cells has $\zeta=4$ neighboring cells with common sides and, therefore, the island distribution can be described in analogy with the problem of percolation over lattice sites in a square lattice. An island is isolated if no other islands are placed in the four neighboring cells with common sides. Two islands have contacts and can be considered islands of larger size if they occupy two cells with a common side. If the distribution of islands is random the fraction of isolated islands is

$$n_1 = Nc(1-c)^{\zeta}. \tag{9}$$

Then all the other islands,

$$n_{com} = (n-n_1) = Nc[1-(1-c)^{\zeta}], \tag{10}$$

form complexes consisting of two and more cells with islands. Therefore, at $c=0.1$ more than 30% of islands form complexes or islands of a larger size. Taking into account that at a concentration c far below the percolation threshold most of these complexes contains two and three unit islands, we can conclude that the number of isolated unit islands and of their complexes is comparable.

A larger number of complexes arise in a lattice built of hexagons where the number of neighboring hexagons ζ is equal to six. At the same value of $c=0.1$, about half of the islands will form complexes.

The other possibility to form the islands of complex shape is to build it from randomly distributed overlapping disks of equal size. The number of disks which form the complexes at the same concentration of disks constitutes also about 30%.

Another reason for the physical nature of the formation of island complexes can be caused by the process of diffusion limited aggregation. Some preliminary experiments indicate that the thermal annealing of InGaN samples after the growth processes[63] or the increase of the growth interruption time before the cap layer deposition in ZnSe/CdSe/ZnSe system[51] drastically affects the number and the distribution of islands on sizes. These facts give the evidence of an important role of the diffusion processes in island formation.

It is known that diffusion limited aggregation leads to a complex disordered shape of aggregates.[62] One of the important features of such aggregates is a multibranch structure around the common center. The average number of branches in an aggregate is restricted by topological considerations and in two-dimensional (2D) systems it is about six. The most part of atoms are in branches, which are well isolated from each other by the distances comparable with the size of branches. Then every branch of the aggregate can be treated as a separate island which is weakly connected with the others through the center.

Schematically, the formation of complex islands due to weak overlapping of the island potential wells which is followed by the metastable states occurrence is shown in Fig. 6(a). A statistical origin of islands suggests a great variety of their realizations. Differences in the size, shape, and concentration of components of the solid solution make it impractical to discuss the properties of excitons in any particular island. In this section we present the model of an average unit island which characterizes an island ensemble and which describes most important optical characteristics of an island ensemble in a 2D quantum well. We assume that clustering together of the unit islands does not change such characteristics of the island ensemble as the DOS and the spectral DOS. However, a complicated spatial shape of combined islands creates the metastable states. We discuss also the mechanism of the fast increasing of the relaxation rate of metastable states at the temperature increase and present results of model calculations.

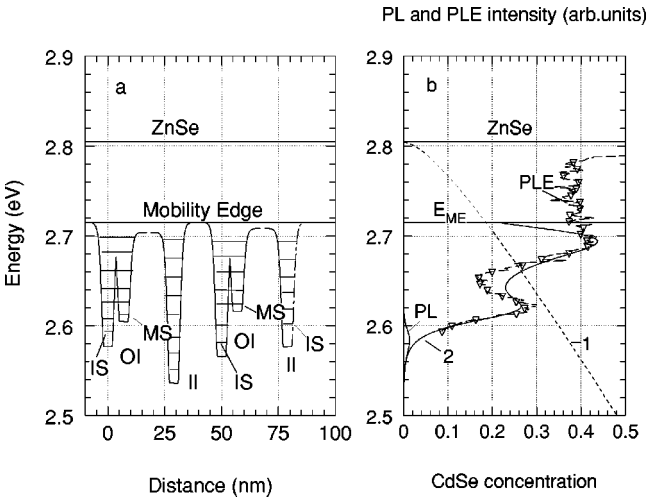

FIG. 6. (a) Energy diagram of a $Zn_{1-x}Cd_xSe$ quantum well in ZnSe. Isolated (II) and overlapping (OI) islands. Metastable states (MS) in overlapping islands and isolated (ground) states (IS) of islands. (b) Curve 1 presents the sum of size quantization energies of electron and hole in quantum well. Curve 2 is the spectral density of the exciton states in quantum well averaged over island ensemble. For comparison the PL and PLE spectra of the sample *Mbe*1 are also given.

B. Model density of states and spectral density of states

We consider the problem of exciton localization in islands of superthin QWs using as a starting point the exciton Hamiltonian for nondegenerate and isotropic bands of Ref. 64. Data on high-resolution transmission electron microscopy for our samples show that the Cd distribution in the growth direction z is more or less symmetrical with respect to the middle point of the QW.[13,14,18] We approximate this distribution by the function

$$C(z,\vec{r}) = \frac{4C(\vec{r})}{[\exp(-z/l)+\exp(z/l)]^2}, \tag{11}$$

where $z=0$ corresponds to the middle point of the distribution. A parameter l defines the width of the Cd distribution, and $C(\vec{r})$ is the Cd concentration in the central monolayer of the QW in the arbitrary point $\vec{r}$ of the lateral plane. The variable $C(\vec{r})$ in Eq. (11) is considered as a continuous function and represents the two dimensional Cd concentration. Using the Cd distribution $C(z,\vec{r})$, we can present the potential perturbation for electrons and for holes produced by a QW in the ZnSe matrix as

$$U(z,\vec{r}_{e,h}) = -C(z,\vec{r}_{e,h})\Delta_{e,h}, \tag{12}$$

where z is the electron or the heavy hole coordinate in the transverse direction, and Δ_e and Δ_h are the electron and hole band offsets, respectively. We assume that

$$\Delta_e + \Delta_h \approx E_g(\mathrm{ZnSe}) - E_g(\mathrm{CdSe}). \tag{13}$$

The ratio $\Delta_e:\Delta_h = 4:1$ and the value $\Delta_e+\Delta_h = 1$ eV will be used in the calculations.

We consider the limit of strong confinement of both particles in the z direction and a large size of an island as compared with the exciton radius in the lateral plane. The eigenfunction of the electron-hole pair can be written as

$$\Phi(\vec{r}_e,\vec{r}_h)=\Psi(\vec{R})\psi(\vec{\rho})\phi(z_e)\phi(z_h). \tag{14}$$

Here, $\vec{R}$ is the 2D dimensional coordinate of the electron-hole pair center of mass, and $\vec{\rho}$ is the space separation of the particles in lateral plane, z_e and z_h are their coordinates in the transverse direction. The strong confinement suggests that radii of both functions $\phi(z_e)$ and $\phi(z_h)$ are less than the exciton Bohr radius a_B for confined particles. In turn, the exciton radius a_B is assumed to be less than the lateral size of an island and to be less than the radius of the wave function $\Psi(\vec{R})$. The last assumption means that the function $C(\vec{r}_{e,h})$ can be considered as the function of the center-of-mass coordinate $C(\vec{R})$ in the lateral plane with appropriate accuracy.

The ground quantization levels for the electron and the hole in the QW with profile in the z direction given by Eq. (11) can be found as eigenvalues of equation

$$\left\{\frac{\hbar^2}{2M_{e,h}}\nabla_z^2-U(z,\vec{R})\right\}\phi(z)=E_{e,h}(\vec{R})\phi(z). \tag{15}$$

Here, $M_{e,h}$ is the electron or the hole mass of the bulk ZnSe. The heavy hole mass M_h we obtain by subtraction of the electron mass $M_e=0.16m_0$ from the translation exciton mass in the (100) direction $M_{hhe}=2.2m_0$.[65] The center-of-mass coordinate $\vec{R}$ enters Eq. (15) as a parameter. The distribution in z direction given by Eq. (11) allows us to obtain an analytical solution of Eq. (15),

$$E_{e,h}(\vec{R})=-\frac{E^0_{e,h}}{4(l/a)^2}\{-1+\sqrt{1+\mathcal{F}}\}^2, \tag{16}$$

where

$$\mathcal{F}=\frac{4C(\vec{R})\Delta_{e,h}}{E^0_{e,h}}\left(\frac{l}{a}\right)^2.$$

a is the interatomic distance, $E^0_{e,h}=\hbar^2/2M_{e,h}a^2$. The corresponding wave functions are

$$\phi_{e,h}(z_{e,h}))\sim[1-\tanh^2(z_{e,h}/l)]^{\mathcal{F}_1}, \tag{17}$$

where $\mathcal{F}_1=\sqrt{-E_{e,h}(\vec{R})/E^0_{e,h}(l/a)^2}$. Equation (16) expresses the size quantization energies using the band edge of the wide gap material as the point of reference.

To describe the island, we introduce a deviation of the Cd distribution from the concentration C_0 corresponding to the mobility edge energy

$$C(\vec{R})=C_0+\delta C(\vec{R}). \tag{18}$$

The strong confinement suggests the dependence of the Coulomb energy on the confinement depth. We can find the Coulomb binding energy $Ry[C(\vec{R})]$ of the quasi-2D exciton and the wave function $\psi(\rho)$ using the Coulomb energy of the electron-hole interaction in the form

$$-\frac{e^2}{\varepsilon_0[C(\vec{R})]}\int\int dz_e dz_h\frac{|\phi(z_e)\phi(z_h)|^2}{\sqrt{\rho^2+(z_e-z_h)^2}},$$

where $\phi(z_{e,h})$ are the normalized wave functions of the electron and the hole confined in the QW. $\varepsilon_0[C(\vec{R})]$ is the static dielectric function which we define as the linear combination of those for ZnSe and CdSe $\varepsilon_0[C(\vec{R})]=C(\vec{R})\varepsilon_0^{CdSe}+[1-C(\vec{R})]\varepsilon_0^{ZnSe}$. The quantization energy $E_1(C)=E_e(C)+E_h(C)+Ry[C]$ as a function of CdSe concentration is given by curve 1 in Fig. 6(b).

Taking now the value $E_1(C_0)=E_e(C_0)+E_h(C_0)+Ry[C_0]$ as the zero point for the energy, we introduce the deviation

$$\delta E(\vec{R})=E_1(C_0+\delta C(\vec{R}))-E_1(C_0)+Ry[C_0+\delta C(\vec{R})]-Ry[C_0], \tag{19}$$

which describes the lateral relief of the island potential energy for the exciton center of mass as a function of the Cd distribution. We note that, in general, the exciton binding energy $Ry[C(\vec{R})]$ is dependent on $\delta C(\vec{R})$ and is also a functional of the electron and hole confinement energies. However, in the case of the sample $Mbe1$ the quasi-2D Coulomb energy depends mainly on $\delta C(\vec{R})$ and only weakly changes from E_{ME} to E_{PL}^{max} because of the strong confinement.

To find the parameters of the lateral profile of the potential well governing the oscillator strength distribution over the levels with different depth, we consider the model potential $\delta E_1(R=|\vec{R}|)$ corresponding to the following deviations of the Cd concentration $\delta C(R)$,

$$\delta C(R)=\Theta(R_1-R)+\Theta(R-R_1)\delta C_{max}/\cosh^2[(R-R_1)/R_2], \tag{20}$$

where $\Theta(X)$ is the steplike theta function, and R_1 and R_2 are parameters which transform the profile of the potential well from a boxlike shape to bell-like or basinlike shapes.[32] Finally, the equation of motion for the center of mass of the exciton in the lateral plane can be written as

$$\left\{\frac{1}{2M}\nabla^2_{\vec{R}}+\delta E(R)\right\}\Psi(\vec{R})=E\Psi(\vec{R}), \tag{21}$$

where $\delta E(R)$ is given by Eqs. (19) and (20).

C. Results of model calculations of the DOS and spectral DOS

The absorption coefficient is proportional to the spectral DOS of excitons localized in islands. In order to find the spectral DOS, we have to evaluate the probability $|\Psi(\vec{\kappa})|^2$, where $\Psi(\vec{\kappa})$ is the Fourier transformation of the wave function $\Psi(\vec{r})$,

$$\Psi(\vec{\kappa}) = \frac{1}{2\pi}\int d^2R \exp\{-i(\vec{\kappa}\vec{R})\}\psi(\vec{R}), \tag{22}$$

in the limit $\kappa \to 0$. We have assumed the average potential profile of Eq. (20) which depends only on the radial variable $|\vec{R}|$. Hence, only the states with the quantum number $m=0$ at arbitrary values of principal quantum number n can contribute to the spectral DOS.

The PLE experimental data on the spectral DOS given by curves 1 and 1′ for the sample $Mbe1$ in Fig. 1 can be approximated best of all by the spectral DOS (curve 5) for the basinlike distribution $\delta C(R)$ given by Eq. (20) with parameters $l/a=5.5$, $R_2/R_1=0.25$, and $\delta C_{max}=0.1425$. The same data are presented in Fig. 6(b). The Cd concentration between the islands is supposed to be $C_0=0.175$ in accordance with the position of E_{ME}. The number of lattice sites covered by the island given by the integral $\pi[\int_0^\infty(\delta C(R)/\delta C_{max})dR]^2 \approx 550$ yields the linear size of island of about 6.5 nm. The distribution of Eq. (20) with given above parameters corresponds to the maximum Cd concentration equal to 31.75% in the center of island and to an exponential decrease of the concentration to the periphery up to 17.5%. Both values are in good accordance with the HR-TEM estimation of these concentrations, 27% and 17%, respectively. The DOS (curve 4 in Fig. 1) has a steplike shape, as can be expected for a 2D system.

Islands of 5–10-nm size can have a considerable number of localized states differing in localization energy. Therefore, we have to sum over all localized states to obtain the spectral DOS. In order to simulate the experimental PLE spectra we must take into account, in general, three inhomogeneous broadening mechanisms of the spectral DOS of the island ensemble, namely, fluctuations of the island size, fluctuations of the maximal Cd content δC_{max}, and fluctuations of Cd and Zn distributions over the lattice sites in an island at the fixed size and δC_{max}. We restrict ourselves to a single-mode island ensemble and take into account fluctuations of δC_{max} and of atom distributions inside the island. The spectral DOS averaged over these parameters is shown by the curve 5 in Fig. 1 and by curve 2 in Fig. 6.

D. Relaxation due to phonon assisted processes

Usually, the exciton-phonon relaxation rate is high enough to maintain an equilibrium or quasiequilibrium population of the exciton states during the radiative recombination time. A special situation arises if the radiative lifetime and the time characterizing relaxation processes for a number of emitting states are comparable. When the rate of exciton-phonon transitions has a strong temperature dependence a complex interplay of these processes can occur. The S-shaped temperature shift of the PL band maximum can be considered as a result of such an interplay. The S-shaped temperature shift can occur for samples containing islands of a complicated space configuration.

The probability of the phonon assisted transition from the state E_λ to the state $E_{\lambda'}$ for $E_\lambda > E_{\lambda'}$ can be written in the second order of the perturbation theory as

$$w_{\lambda,\lambda'} = \frac{2\pi}{\hbar}\frac{v_0}{(2\pi)^3}\int d^3q |H_{\lambda,\lambda'}(j,q)|^2 \delta(E_\lambda - E_{\lambda'} - \hbar\Omega_{j,q}) \times [1+N(\Omega_{j,q})]. \tag{23}$$

In the opposite case $E_\lambda < E_{\lambda'}$, the phonon energy $\hbar\Omega_{j,q}$ in the δ function changes its sign and the phonon Bose factor $N(\Omega_{j,q})$ appears instead of $[1+N(\Omega_{j,q})]$. In Eq. (23) $H_{\lambda,\lambda'}(j,q)$ is the matrix element of exciton interaction with phonon of branch j with wave vector q. As follows from Eq. (23), the energy of a phonon involved in this process should be equal to the energy difference $(E_\lambda - E_{\lambda'})$, and the temperature dependence of the probability arises at temperatures comparable to the energy difference.

The transition of an exciton from a state E_λ to the ground state E_1 and the backward transition $E_1 \to E_\lambda$ maintain an equilibrium population of both states if the radiative lifetime for these states is large enough. The ratio of the equilibrium population of the excited state E_λ and the state E_1 at temperature T is equal to the ratio of phonon Bose factors for these two processes, which, as it follows from energy conservation law, is

$$N(\Omega_{j,q})/[1+N(\Omega_{j,q})] = \exp\{-(E_\lambda - E_1)/T\}. \tag{24}$$

(Here and below the energy units are used for the temperature.) At temperatures $T \ll (E_\lambda - E_1)$ the ground state will be mainly populated while the excited state population reaches a significant value only at $T \approx (E_\lambda - E_1)$.

The situation differs if the equilibrium is maintained between the ground state and a group of $\mathcal{Z}$ states with localization energies E_λ, $\lambda = 2, \ldots (\mathcal{Z}+1)$. We consider the situation when the equilibrium is maintained between the ground state and a group of $\mathcal{Z}$ states with close localization energies E_λ, $\lambda = 2, \ldots (\mathcal{Z}+1)$. In this case for any $\lambda > 1$ the inequality

$$|E_\lambda - \overline{E_\lambda}| \ll (\overline{E_\lambda} - E_1), \tag{25}$$

should hold, where the average energy is

$$\overline{E_\lambda} = \frac{1}{\mathcal{Z}}\left(\sum_{i=2}^{(\mathcal{Z}+1)} E_\lambda\right). \tag{26}$$

The transition probability from the ground state to the $\mathcal{Z}$ states of the group of excited states increases proportionally to $\mathcal{Z}$. As a result, the equilibrium distribution will be reached at the temperature

$$T = \frac{(\overline{E_\lambda} - E_1)}{\ln \mathcal{Z}}, \tag{27}$$

which at $\mathcal{Z}=6$ is almost two times less than the difference $(\overline{E_\lambda} - E_1)$. At the same time the relaxation lifetime for the transition into the ground state remains dependent on the temperature only due to phonons with an energy of order $(\overline{E_\lambda} - E_1)$.

E. Phonon assisted processes in island ensembles

In order to answer the question of why the metastable states disappear from the emission at low temperatures before being thermally populated, we have to consider in a very detail the major features of the exciton-phonon interaction in islands, and to analyze the influence of complex shapes of real islands on the processes of the exciton-phonon interaction.

The exciton-phonon Hamiltonian H_{ef} presents the sum of the electron- and hole-phonon Hamiltonians. The matrix elements of the exciton-phonon Hamiltonian can be written in the effective mass approximation as[66]

$$H^{\alpha,f}_{\Phi\Phi}=[F^{\alpha}_{e,q}\exp i(\vec{q}\vec{r_e})+F^{\alpha}_{h,q}\exp i(\vec{q}\vec{r_h})]_{\Phi\Phi}. \qquad (28)$$

The functions $F^{\alpha}_{e,q}$ and $F^{\alpha}_{h,q}$ were given by Cohen and Sturge[66] for the Frohlich interaction ($\alpha=F$) and for the deformation ($\alpha=D$) and for piezoelectric ($\alpha=P$) coupling to acoustical phonons.

Using Eq. (14) we can write the matrix elements in Eq. (28) as

$$[\exp i(\vec{q}\vec{r_e})]_{\Phi\Phi} =[\exp i(\vec{\xi}\vec{R})]_{\Psi(R)\Psi'(R)} \times\left[\exp\pm i\left(\vec{\xi}\vec{\rho}\frac{\mu}{m_{e,h}}\right)\right]_{\psi(\rho),\psi(\rho)} [\exp i(q_z z)]_{\phi_{e,h}(z)\phi_{e,h}(z)}. \qquad (29)$$

Here, ξ is the phonon wave vector in the plane of the QW, and q_z is its component perpendicular to the QW plane.

Although both diagonal and off-diagonal matrix elements $[\exp i(\vec{\xi}\vec{R})]_{\Psi(R)\Psi'(R)}$ are important we shall take into account only the matrix elements between the ground states $n=1$ of the internal motion of the exciton

$$\left[\exp\pm i\left(\vec{\xi}\vec{\rho}\frac{\mu}{m_{e,h}}\right)\right]_{1,1}$$

and those for the size quantization $[\exp i(q_z z)]_{\phi_{e,h}(z)\phi_{e,h}(z)}$. Here μ is the reduced mass of the exciton.

1. Phonon assisted processes: vanishing of the narrow lines of micro-PL with temperature

The diagonal matrix element $[\exp i(\vec{\xi}\vec{R})]_{\lambda,\lambda}$ in the time-dependent Hamiltonian of the exciton-phonon interaction leads to the formation of a continuum exciton-phonon band. The increase of the width of this band with the temperature is accompanied by the quenching the narrow δ-like zero-phonon line. As a result, instead of a narrow δ-like contribution of the localized state E_λ to the density of states a broad band $\Delta(\hbar\omega-E_\lambda)$ appears. Using well known results from Refs. 67 and 68 we can write the density of states for localized excitons at an arbitrary temperature as

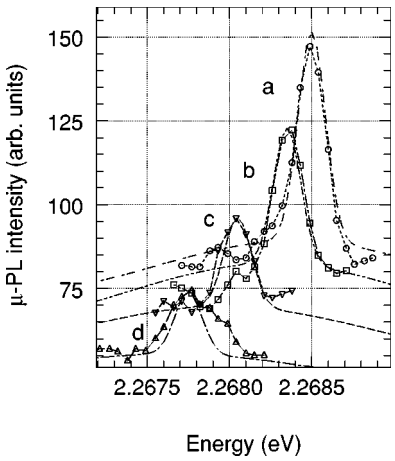

FIG. 7. Reduction of narrow line intensity within the μ-PL band as temperature increases (sample $Mbe1$). Experimental data at $T=7$, 15, 22, and 35 K from *a* to *d*, respectively are presented by lines with symbols. Broken lines are calculated line shapes.

$$\Delta^{\pm}(\hbar\omega-E_\lambda)=\frac{1}{2\pi}\int_{-\infty}^{\infty}dt\exp[i(\omega-E_\lambda/\hbar)t\pm\mathcal{F}_{\lambda,\lambda}(t)], \qquad (30)$$

where

$$\mathcal{F}_{\lambda,\lambda}(t)=\sum_{j,q}\frac{|H_{\lambda,\lambda}(j,\vec{q})|^2}{(\hbar\Omega_{j,q})^2}\{[\exp(-i\Omega_{j,q}t)-1](N(\Omega_{j,q})+1)+[\exp(i\Omega_{j,q}t)-1]N(\Omega_{j,q})\}. \qquad (31)$$

Here, $H_{\lambda,\lambda}(j,\vec{q})$ is the matrix element of the Hamiltonian $H^{\alpha,f}_{\Phi\Phi}$ of Eq. (28) containing only diagonal matrix elements of the operator $[\exp i(\vec{\xi}\vec{R})]$. The wave function of the exciton localized in the island $\Psi_\lambda(R)$ decreases rapidly beyond the island, and, therefore, the island size L or the radius of the wave function restricts the wave vectors of acoustical phonons forming the exciton-phonon band. The sum over q in Eq. (31) is restricted by the values of $q\approx q_0=1/L$, where L is the lateral size of the wave function or of the island. At $L\approx 5$ nm and at the sound velocity $s=1.5\times10^5$ cm/sec the energy of the involved phonon is $\hbar q_0\ s\approx 0.2$ meV. The exciton-phonon interaction rate increases with the temperature because the Bose factors for Stokes and anti-Stokes processes for acoustical phonons reach their classical limit $T/\hbar q_0\ s$. This results in a decrease of the peak intensity of the zero-phonon line as

$$\exp\left\{-\sum_{j,q}\frac{|H_{\lambda,\lambda}(j,\vec{q})|^2}{(\hbar\Omega_{j,q})^2}[2N(\Omega_{j,q})+1]\right\} \approx\exp[-2g_0(T/\hbar q_0 s)], \qquad (32)$$

where g_0 is the effective constant of exciton-phonon interaction.

Figure 7 demonstrates the effect of this part of exciton-phonon interaction on the narrow line peak intensity in the micro-PL spectrum of $Zn_{1-x}Cd_xSe$ QW $Mbe1$. The phonon wings of the narrow line are more difficult to observe since

they are hidden in a much more strong background due to phonon replicas of higher states of the islands. The temperature interval where the peak intensity decreases dramatically is defined by the energy of the acoustical phonon forming the exciton-phonon band and, therefore, by the size of the typical island or the wave function of exciton in a QW. In agreement with experiment, the decrease of the narrow line intensity is about five times at the value of $\hbar q_0 \ s \approx 0.2$ meV, and at $g_0 \approx 0.045$ within the temperature interval presented in Fig. 7.

2. Relaxation processes with diagonal interaction in all orders of perturbation theory

We assume that due to the space separation of interacting metastable states an inequality $(w_{\lambda,\lambda'}\tau_{em}) \ll 1$ holds.

The probability $w_{\lambda,\lambda'}$ given by Eq. (23) is proportional to the phonon DOS $g_j(\hbar\omega)$ at the energy $\hbar\omega = E_\lambda - E_{\lambda'}$ reduced by the factor $|H_{\lambda,\lambda'}(j,q)|^2$. The energy conservation law restricts the energy of the phonon participating in the process while the large spatial extent of island restricts the maximum values of the phonon wave vectors. We will show that multiphonon corrections due to diagonal matrix elements $H_{\lambda,\lambda}(j,q)$ can strongly increase the value of $w_{\lambda,\lambda'}$.

Straightforward calculations taking into account the renormalization of both states λ and λ' and the exchange of phonons between these two states due to the diagonal matrix element of the exciton-phonon interaction transform Eq. (23) into

$$w_{\lambda,\lambda'} = \frac{2\pi}{\hbar}\frac{v_0}{(2\pi)^3}\int d^3q |H_{\lambda,\lambda'}(j,q)|^2 [1 + N(\Omega_{j,q})] \sum_{m=0}^{\infty}\sum_{l=0}^{m}\frac{1}{(m-l)!\,l!} \times \left[\prod_{\alpha=0}^{m-l}\sum_{j_\alpha,q_\alpha} g^{+}_{\lambda,\lambda'}(j_\alpha,\vec{q}_\alpha)\right] \times \left[\prod_{\beta=0}^{l}\sum_{j_\beta,q_\beta} g^{-}_{\lambda,\lambda'}(j_\beta,\vec{q}_\beta)\right]\delta \times \left[E_{\lambda,\lambda'} - \hbar\Omega_{j,q} - \sum_{\alpha=0}^{m-l}\hbar\Omega_{j_\alpha,q_\alpha} + \sum_{\beta=0}^{l}\hbar\Omega_{j_\beta,q_\beta}\right], \tag{33}$$

where

$$g^{+}_{\lambda,\lambda'}(j,\vec{q}) = (N(\Omega_{j,q})+1)\left|\frac{H_{\lambda,\lambda}(j,\vec{q})}{(\hbar\Omega_{j,q})} + \frac{H_{\lambda',\lambda'}(j,\vec{q})}{(\hbar\Omega_{j,q})}\right|^2, \tag{34}$$

and $g^{-}_{\lambda,\lambda'}(j,\vec{q})$ is obtained by the substitution of $N(\Omega_{j,q})$ instead of $[N(\Omega_{j,q})+1]$.

The zeroth term of this series at $m=0$, $l=0$, $\alpha=0$, and $\beta=0$ coincides exactly with Eq. (23). As follows from Eq. (34), the exciton-phonon constants are, practically, doubled because both initial λ and final λ' states are renormalized by the diagonal exciton-phonon interaction and by the exchange of phonons. The argument of the δ function in Eq. (33) shows the major effect which results from the diagonal exciton-phonon interaction. That is, it shows that in the relaxation process due to the off-diagonal exciton-phonon interaction an a arbitrary number of phonons with small energies can be involved.

This leads to an increase of the relaxation probability as compared with Eq. (23), and to the strong temperature dependence of the probability at low temperature. The last result follows from Eq. (34), because the exciton phonon interaction increases with temperature. Taking into account that the most important phonons have wave vectors of the order of $q \approx L^{-1}$, where L is the spatial size of the exciton localized in an island, we conclude that the Bose factors due to the diagonal matrix elements are already proportional to T at very low temperature.

In order to estimate the temperature dependence of the relaxation probability, we keep in Eq. (33) only the Stokes processes with emission of phonons. This leads to the simplification of Eq. (33):

$$w_{\lambda,\lambda'} = \frac{2\pi}{\hbar}\frac{v_0}{(2\pi)^3}\int d^3q |H_{\lambda,\lambda'}(j,q)|^2 [1 + N(\Omega_{j,q})] \sum_{m=0}^{\infty}\frac{1}{m!}\left[\prod_{\alpha=0}^{m}\sum_{j_\alpha,q_\alpha} g^{+}_{\lambda,\lambda'}(j_\alpha,\vec{q}_\alpha)\right] \times \delta\left[E_{\lambda,\lambda'} - \hbar\Omega_{j,q} - \sum_{\alpha=0}^{m}\hbar\Omega_{j_\alpha,q_\alpha}\right]. \tag{35}$$

Here, the wave vectors of all m phonons are small $q_\alpha \sim q_0 \approx L^{-1}$. Assuming the inequality $T \gg \hbar s q_0$, where s is the sound velocity, and performing the integration over q with the help of the δ function, we obtain

$$w_{\lambda,\lambda'} \approx \frac{2\pi}{\hbar}\frac{v_0}{2\pi^2}\sum_{m=0}^{\infty}\frac{1}{m!}\left[\frac{4g_0T}{\hbar s q_0}\right]^m |H_{\lambda,\lambda'}[j,Q(m)]|^2 [1 + N(\Omega_{j,Q(m)}]Q^2(m), \tag{36}$$

where

$$Q(m) = [E_{\lambda,\lambda'} - m\hbar q_0 s]/(\hbar s).$$

In Eq. (36) we have used the same simplified expression for the exciton-phonon interaction constant g_0, as earlier in Eq. (32). As follows from Eq. (36), the magnitude of the exciton-phonon interaction constant is doubled as compared with Eq. (32). The value of the terms in the sum of Eq. (36) increases with the m increase when the temperature is high enough and $[4g_0T/(m\hbar s q_0)] > 1$ until the factors decreasing with m, namely, $Q^2(m)$ and $|H_{\lambda,\lambda'}[j,Q(m)]|^2$, become more important. The value of m is restricted by the inequality $m \leq E_{\lambda,\lambda'}/\hbar q_0 s$. Therefore, it is possible to find an optimal value of $m = m_0$, which defines, at a given temperature, the value of $w_{\lambda,\lambda'}$ and its temperature increase

$$w_{rel}(T) \approx w_{\lambda,\lambda'}(0)\{1 + [(4g_0T)/(m_0\hbar s q_0)]^{m_0}\}. \tag{37}$$

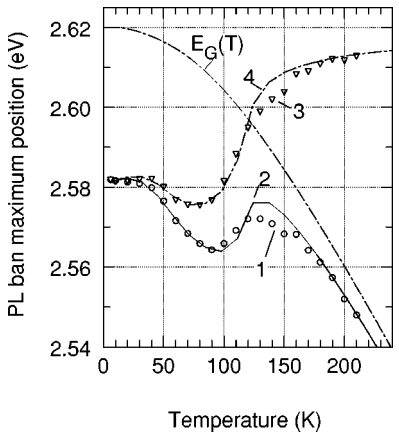

FIG. 8. The temperature shift of the PL band maximum of the sample $Mbe1$ (symbols 1). Curve 2 presents the anomalous model dependence. Open triangles 3 are the experimental data after subtraction of the gap shift $\Delta E_G(T)$, curve 4 gives results of calculation without $\Delta E_G(T)$.

The same consideration can be used for any state λ_i from the group of states nearest to the ground state. If the lifetimes of these states at low temperatures are much shorter or even comparable to the radiative time, they can participate in the formation of the PL band. The temperature increase will change the situation and at some temperature the relaxation probability will exceed the emission probability. As a result, the shape of the PL band will change.

F. Model calculation of the shift of the PL band maximum

The population of the localized states at finite temperatures was found by means of Eq. (6) after substitution of $\rho_{isol+mts}(\omega,T)$ for $\rho_{isol}(\omega)$. The detailed comparison of the experimental shift with results of calculations for the sample $Mbe1$ is presented in Fig. 8. The fitting shows that $w_{rel}(T)\approx w_{\lambda,\lambda'}(0)[(4g_0/m_0)(T/\hbar q_0 s)]^{m_0}$ leads to the acceptable coincidence with the experimental temperature shift of the PL maximum in the low temperature region with the parameters $m_0=3.5-3.7$, $(w_{\lambda,\lambda'}(0)\tau_{em})=0.1$, and at the same value of $g_0\approx 0.045$ which has been used in estimation of narrow lines quenching.

V. SUMMARY

We have studied the temperature dependences of the PL band maximum for 2D ultrathin QWs both in random and inhomogeneous solid solutions with highly mismatched components. In the latter case the nanoislands enriched by the narrow gap component of the solid solution cause a deep localization of excitons. We have demonstrated that the anomalous temperature dependence of the PL band maximum position is a consequence of the relaxation of metastable states which form a considerable part of the PL band at low temperatures. The properties of metastable states reflect a complex island structure which can be due to the formation of statistical clusters of the islands or can be caused by the diffusion limited process of the island growth. The exciton-phonon interaction leads, on the one hand, to the relaxation of excited excitons followed by their thermalization, and, on the other hand, results in a homogeneous broadening of exciton bands. The mechanism of exciton-phonon interaction responsible for the fast decrease of the lifetime of metastable states with increasing temperature has much in common with the one leading to quenching of the narrow lines in μ-PL. The obtained results show that the temperature shift of the PL-band maximum can be used for the characterization of the island ensemble.

ACKNOWLEDGMENTS

The authors are pleased to thank I. Sedova and S. Sorokin for providing the MEE samples, and E. Kurtz and M. Gruen for providing the MBE samples. It is also a pleasure to thank D. Litvinov, A. Rosenauer, and D. Gerthsen for the HRTEM data and valuable discussions. This work was partly supported by the Center for Functional Nanostructures of the Deutsche Forschungsgemeinschaft within project A2, by the Russian Programs ''Physics of Solid State Nanostructures,'' by the Russian Academy of Sciences through the program ''Low Dimensional Quantum Structures,'' and by Russian Foundation for Basic Research.

*Permanent address: Petersburg Nuclear Physics Institute, 188350, St. Peterburg, Russia.

†Permanent address: A.F. Ioffe Physical-Technical Institute, 194021, St. Petersburg, Russia.

[1] S.A. Permogorov in *Excitons*, edited by E.I. Rashba and M.D. Sturge (North-Holland, Amsterdam, 1982), Pt. 5

[2] S.A. Permogorov and A.N. Reznitsky, J. Lumin. **52**, 201 (1992).

[3] A. Klochikhin, A. Reznitsky, S. Permogorov, T. Breitkopf, M. Grun, M. Hetterich, C. Klingshirn, V. Lyssenko, W. Langbein, and J.M. Hvam, Phys. Rev. B **59**, 12947 (1999).

[4] D. Bimberg, M. Grudmann, and N.N. Ledentsov, *Quantum Dot Heterostructures* (Wiley, New York, 1998).

[5] F. Flack, N. Samarth, V. Nikitin, P.A. Crowell, J. Shi, J. Levy, and D.D. Awschalom, Phys. Rev. B **54**, R17312 (1996).

[6] S.V. Ivanov, A.A. Toropov, T.V. Shubina, S.V. Sorokin, A.V. Lebedev, I.V. Sedova, and P.S. Kop'ev, J. Appl. Phys. **83**, 3168 (1998).

[7] S. Sorokin, T. Shubina, A. Toropov, I. Sedova, A. Sitnikova, R. Zolotareva, S. Ivanov, and P. Kop'ev, J. Cryst. Growth **201/202**, 461 (1999).

[8] R.N. Kyutt, A.A. Toropov, S.V. Sorokin, T.V. Shubina, S.V. Ivanov, M. Karlsteen, and M. Willander, Appl. Phys. Lett. **75**, 373 (1999).

[9] M. Strassburg, Th. Deniozou, A. Hoffmann, R. Heitz, U.W. Pohl, D. Bimberg, D. Litvinov, A. Rosenauer, D. Gerthsen, S. Schwedhelm, K. Lischka, and D. Schikora, Appl. Phys. Lett. **76**, 685 (2000).

[10] H. Kirmse, R. Schneider, M. Rabe, W. Neumann, and F. Henneberger, Appl. Phys. Lett. **72**, 1329 (1998).

[11] T. Kümmell, R. Weigand, G. Bacher, A. Forchel, K. Leonardi, D.

Hommel, and H. Selke, Appl. Phys. Lett. **73**, 3105 (1998).
[12] D. Schikora, S. Schweldhelm, D.J. As, K. Lishka, D. Litvinov, A. Rosenauer, D. Gerthsen, M. Strassburg, A. Hoffmann, and D. Bimberg, Appl. Phys. Lett. **76**, 418 (2000).
[13] D. Litvinov, A. Rosenauer, D. Gerthsen, and N.N. Ledentsov, Phys. Rev. B **61**, 16819 (2000).
[14] N. Peranio, A. Rosenauer, D. Gerthsen, S.V. Sorokin, I.V. Sedova, and S.V. Ivanov, Phys. Rev. B **61**, 16015 (2000).
[15] E. Kurtz, M. Schmidt, M. Baldauf, D. Litvinov, D. Gerthsen, H. Kalt, and C. Klingshirn, Phys. Status Solidi B **224**, 185 (2001).
[16] C.S. Kim, M. Kim, J.K. Furdina, M. Dobrowolska, S. Lee, H. Rho, L.M. Smith, Howard E. Jackson, E.M. James, Y. Xin, and N.D. Browining, Phys. Rev. Lett. **85**, 1124 (2000).
[17] E. Kurtz, M. Schmidt, M. Baldauf, S. Wachter, M. Grün, H. Kalt, C. Klingshirn, D. Litvinov, A. Rosenauer, and D. Gerthsen, Appl. Phys. Lett. **79**, 1118 (2001).
[18] E. Kurtz, B. Dal Don, M. Schmidt, H. Kalt, C. Klingshirn, D. Litvinov, A. Rosenauer, and D. Gerthsen, Thin Solid Films **412**, 89 (2002).
[19] K. Leonardi, H. Selke, H. Heinke, K. Ohkawa, D. Hommel, F. Gindele, and U. Woggon, J. Cryst. Growth **184/185**, 259 (1998).
[20] T. Passow, H. Heike, T. Schmidt, J. Falta, A. Stockmann, H. Selke, P.L. Ryder, K. Leonardi, and D. Hommel, Phys. Rev. B **64**, 193311 (2001).
[21] T. Passow, K. Leonardi, H. Heinke, D. Hommel, D. Litvinov, A. Rosenauer, D. Gerthsen, J. Seufert, G. Bacher, and A. Forchel, J. Appl. Phys. **92**, 6546 (2002).
[22] M. Lowisch, M. Rabe, F. Keller, and F. Henneberger, Appl. Phys. Lett. **74**, 2489 (1999).
[23] S. Lee, J.C. Kim, H. Rho, C.S. Kim, L.M. Smith, Howard E. Jackson, J.K. Furdina, and M. Dobrowolska, Phys. Rev. B **61**, R2405 (2000).
[24] J. Puls, M. Rabe, H.-J. Wünsche, and F. Henneberger, Phys. Rev. B **60**, R16303 (1999).
[25] F. Gindele, U. Woggon, W. Langbein, J.M. Hvam, K. Leonardi, D. Hommel, and H. Selke, Phys. Rev. B **60**, 8773 (1999).
[26] V. Türck, S. Rodt, O. Stier, R. Heitz, R. Engelhardt, U.W. Pohl, D. Bimberg, and R. Steingrüber, Phys. Rev. B **61**, 9944 (2000).
[27] L. Rho, L.M. Robertson, L.M. Smith, Howard E. Jackson, S. Lee, M. Dobrowolska, and J.K. Furdina, Appl. Phys. Lett. **77**, 1813 (2000).
[28] L. Rho, L.M. Smith, H.E. Jackson, S. Lee, M. Dobrowolska, and J.K. Furdina, Phys. Status Solidi B **224**, 165 (2001).
[29] M. Strassburg, M. Dworzak, H. Born, R. Heitz, A. Hoffmann, M. Bartels, K. Lischka, D. Schikora, and J. Christen, Appl. Phys. Lett. **80**, 473 (2002).
[30] A. Reznitsky, A. Klochikhin, S. Permogorov, L. Tenishev, I. Sedova, S. Sorokin, S. Ivanov, M. Schmidt, H. Zhao, E. Kurtz, H. Kalt, and C. Klingshirn, Phys. Status Solidi B **229**, 509 (2002).
[31] A. Reznitsky, A. Klochikhin, S. Permogorov, in *Spectroscopy of Systems with Spatially Confined Structures*, edited by Baldasare di Bartolo (Kluwer, Dordrecht, 2002), p. 419.
[32] A. Klochikhin, A. Reznitsky, S. Permogorov, I. Sedova, S. Sorokin, S. Ivanov, D. Litvinov, D. Gerthsen, B. Dal Don, H. Priller, H. Kalt, and C. Klingshirn, in *Proc. of 11-th Intern. Symp. "Nanostructures: Physics and Technology," St. Petersburg, Russia* (Ioffe Institute, St. Petersburg, 2003), p. 206.
[33] M.S. Skolnik, P.R. Tapster, S.J. Bass, A.D. Pitt, N. Apsley, and S.P. Aldred, Semicond. Sci. Technol. **1**, 29 (1986).
[34] S.T. Davey, E.G. Scott, B. Wakefield, and G.J. Davies, Semicond. Sci. Technol. **3**, 365 (1988).
[35] M. Gurioli, A. Vinattieri, J. Martinez-Pastor, and M. Colocci, Phys. Rev. B **50**, 11817 (1994).
[36] Mitsuru Sugawara, Phys. Rev. B **51**, 10743 (1995).
[37] E.M. Daly, T.J. Glynn, J.D. Lambkin, L. Considine, and S. Walsh, Phys. Rev. B **52**, 4696 (1995).
[38] A. Polimeni, A. Patane, M. Grassi Alessi, M. Capizzi, F. Martelli, A. Bosacchi, and S. Franchi, Phys. Rev. B **54**, 16389 (1996).
[39] Y.-H. Cho, G.H. Gainer, A.J. Fischer, J.J. Song, S. Keller, U.K. Mishra, and S.P. DenBaars, Appl. Phys. Lett. **73**, 1370 (1998).
[40] W.V. Lundin, A.S. Usikov, A.V. Sakharov, V.V. Tretyakov, D.V. Poloskin, N.N. Ledentsov, and A. Hoffmann, Phys. Status Solidi A **176**, 379 (1999).
[41] Q. Li, S.J. Xu, W.C. Cheng, M.H. Xie, S.Y. Tong, C.M. Che, and H. Yang, Appl. Phys. Lett. **79**, 1810 (2001).
[42] M. Grassi Alessi, F. Fragano, A. Patane, M. Capizzi, E. Runge, and R. Zimmermann, Phys. Rev. B **61**, 10985 (2000).
[43] H.D. Sun, M. Hetterich, M.D. Dawson, A.Yu. Egorov, D. Bernklau, and H. Riechert, J. Appl. Phys. **92**, 1380 (2002).
[44] S. Wachter, B. Dal Don, M. Schmidt, M. Baldauf, A. Dinger, E. Kurtz, C. Klingshirn, and H. Kalt, Phys. Status Solidi B **224**, 437 (2001).
[45] H.-P. Tranitz, H.P. Wagner, R. Engelhardt, U.W. Pohl, and D. Bimberg, Phys. Rev. B **65**, 035325 (2002).
[46] A. Reznitsky, A. Klochikhin, H. Priller, B. Dal Don, G. Schwartz, H. Zhao, H. Kalt, C. Klingshirn, S. Permogorov, L. Tenishev, I. Sedova, S. Sorokin, and S. Ivanov, Phys. Status Solidi C **238**, 1544 (2003).
[47] H.-C. Ko, D.-C. Park, Y. Kawakami, S. Fujita, S. Fujita, and Y.-S. Kim, Appl. Phys. Lett. **73**, 1388 (1998).
[48] A. Dinger, M. Badlauf, S. Petillon, A. Hepting, D. Lüerssen, M Gün, H. Kalt, and C. Klingshirn, J. Cryst. Growth **214/215**, 660 (2000).
[49] B. Dal Don, E. Tsitsishvili, H. Kalt, K. Kohary, R. Eichmann, S.D. Baranovskii, and P. Thomas, Phys. Status Solidi C **238**, 1509 (2003).
[50] J.C. Kim, H. Rho, L.M. Smith, Howarde. Jackson, S. Lee, M. Dobrowolska, and J.K. Furdina, Appl. Phys. Lett. **75**, 214 (1999).
[51] E. Kurtz, M. Schmidt, M. Baldauf, S. Wachter, M. Grün, D. Litvinov, S.K. Hong, J.X. Shen, T. Yao, D. Gerthsen, H. Kalt, and C. Klingshirn, J. Cryst. Growth **214/215**, 712 (2000).
[52] L. Vina, S. Logothetidis, and M. Cardona, Phys. Rev. B **30**, 1979 (1984), and references therein.
[53] M. Cardona, Phys. Status Solidi B **188**, 1209 (2001).
[54] D. Luerssen, R. Bleher, and H. Kalt, Phys. Rev. B **61**, 15812 (2000).
[55] Y.P. Varshni, Physica (Amsterdam) **34**, 149 (1967).
[56] M. Quintero, C. Rincon, R. Tovar, and J.C. Woolley, J. Phys.: Condens. Matter **4**, 1281 (1992).
[57] A. Manoogian and A. Leclerc, Can. J. Phys. **57**, 1766 (1979).
[58] K.P. O'Donnell and X. Chen, Appl. Phys. Lett. **58**, 2924 (1991).
[59] R. Pässler, J. Appl. Phys. **83**, 3356 (1998).
[60] *Landolt-Börnstein: Numerical Data*, New Series, Group III, Vol. 17, Subvolume b, edited by O. Madelung (Springer-Verlag, Berlin, 1982), p. 151.
[61] S.W. Haan and R. Zwanzig, J. Phys. A **10**, 1547 (1977).

[62] *Fractals in Physics*, edited by L. Pietronero and E. Tesatti (North Holland, Amsterdam, 1986).
[63] A.V. Sakharov, W. Lundin, I.L. Krestnikov, E.E. Zavarin, A.S. Usikov, A.F. Tstsul'nikov, N.N. Ledentsov, A. Hoffmann, D. Bimberg, and Zh.I. Alferov, in *Proc. 8-th Intern. Symp. "Nanostructures: Physics and Technology," St. Petersburg, Russia*, (Ioffe Institute, St. Petersburg, 2000), p. 216.
[64] G. Bastard, E.E. Mendez, L.L. Chang, and L. Esaki, Phys. Rev. B **26**, 1974 (1982).
[65] B. Sermage and G. Fishman, Phys. Rev. Lett. **43**, 1043 (1972).
[66] E. Cohen and M. Sturge, Phys. Rev. B **25**, 3828 (1982).
[67] A.A. Maradudin, Solid State Phys. **18**, 273 (1966); **19**, 1 (1966).
[68] M.H. Pryce, in *Phonons*, edited by R.W.H. Stevenson (Plenum, New York, 1966).